TUDelft

Delft University of Technology

Enhanced corrosion protection of mild steel by the synergetic effect of zinc aluminum polyphosphate and 2-mercaptobenzimidazole inhibitors incorporated in epoxy-polyamide coatings

Mirzakhanzadeh, Z.; Kosari, A.; Moayed, M. H.; Naderi, R.; Taheri, P.; Mol, J. M.C.

Important note
To cite this publication, please use the final published version (if applicable).
Please check the document version above.

Enhanced corrosion protection of mild steel by the synergetic effect of zinc aluminum polyphosphate and 2-mercaptobenzimidazole inhibitors incorporated in epoxy-polyamide coatings

Z. Mirzakhanzadeh[a], A. Kosari[a,b], M.H. Moayed[a,*], R. Naderi[c], P. Taheri[b], J.M.C. Mol[b]

[a] Materials and Metallurgical Engineering Department, Faculty of Engineering, Ferdowsi University of Mashhad, Mashhad 91775-1111, Iran
[b] Department of Materials Science and Engineering, Delft University of Technology, Mekelweg 2, 2628 CD Delft, The Netherlands
[c] School of Metallurgy and Materials Engineering, College of Engineering, University of Tehran, P.O. Box 11155-4563, Tehran, Iran

ARTICLE INFO

ABSTRACT

This work investigates the synergetic effect of zinc aluminum polyphosphate (ZAPP) and 2-mercaptobenzimidazole (MBI) on the corrosion protection of mild steel coated with a solvent-borne epoxy-polyamide layer. The magnitude and trend of electrochemical impedance spectroscopy data over 70-d immersion in 3.5 wt.% NaCl solution indicate superior corrosion protection of the combined inhibitors compared to those containing either just ZAPP or MBI. Pull-off tests show that the combined inhibitor system provides an improved adhesion strength. The enhanced corrosion performance is correlated to precipitation of a protective layer at the coating/metal interface verified by SEM and electrochemical studies upon exposure to electrolytes.

1. Introduction

Organic coatings are used widely to retard corrosion of metal substrates being efficient barriers against ingress of corrosive environments [1–3]. Their corrosion performance can be enhanced by the incorporation of an additional phase compatible with the polymeric matrix [4–7]. In fact, the coatings can also serve as reservoirs for corrosion inhibiting pigments providing an extra protection of the substrates at defects once corrosion starts [8–10]. Epoxy resins are employed extensively as reservoirs of inhibitors in corrosive media such as chloride-containing environments [11–14].

Recent works attempt to incorporate combinations of two or more types of inhibitors in organic coatings to further improve their corrosion protection [13,15–17]. Kallip et al. observed a synergetic inhibition effect on Zn–Fe model samples when an anodic inhibitor, i.e. 1,2,3-benzotriazole, is combined with a cathodic one, i.e. Ce(NO₃)₃ [18]. In another research, Mahdavian and Ashhari added 2-mercaptobenzimidazole and 2-mercaptobenzoxazole to a polyester-melamine coating and observed a synergetic effect in corrosion protection of the coatings due to formation of a protective layer on steel substrate [19]. Balaskas et al. reported an improvement in the barrier properties of silicate–epoxy coatings doped with organic and inorganic inhibitors and applied on Al alloy 2024-T3. However, they observed no significant synergy between $Ce(NO_3)_3$ and 2-mercaptobenzothiazole [20].

Inhibitor selection is an important step towards designing an efficient inhibitor-coating system [13]. Phosphate-based pigments are known as non-toxic inorganic inhibitors used widely for protection of various metal substrates [21,22]. The corrosion inhibition mechanism of polyphosphates is based on the presence of a high phosphate content and chelate building potential with multivalent metal cations [23]. Furthermore, combined polyvalent metals exhibit impeding cationic reactions through deposition of physical protective barriers [24]. Naderi and Attar reported corrosion inhibition provided by zinc aluminum polyphosphate (ZAPP) on mild steel due to the formation of a protective layer, limiting the access of corrosive species to the steel surface [22]. Moreover, 2-mercaptobenzimidazole (MBI) is a known corrosion inhibitor for various metal substrates [25–29]. MBI shows corrosion inhibition of iron in NaCl solution [26] and mild steel in 1 M HCl [28] through an adsorption onto metal surfaces.

In this study, the inhibition performance of combined ZAPP and MBI are examined by incorporating in an epoxy-polyamide coating. Electrochemical measurements are conducted to investigate the corrosion behavior of bare mild steel in 3.5 wt.% NaCl solution containing a mixture of ZAPP and MBI. Moreover, scanning electron microscopy (SEM) and Fourier transform infrared spectroscopy (FTIR) are employed to analyze the surface morphology and chemistry of bare metals exposed to the inhibitor-containing solutions. EIS experiments and pull-off tests are used to assess the water-uptake, barrier, dry and wet

---

Table 1
Chemical composition of the mild steel base substrate.

Grade	Chemical Composition (wt.%)					
	C	Mn	Si	P	S	Fe
ST13	0.07	0.33	0.10	0.022	0.024	Balance

adhesive properties of the inhibitor-doped coatings in 3.5 wt.% NaCl solution.

2. Materials and methods

2.1. Materials

The substrates used in this study were 5 cm × 7 cm × 1 mm mild steel plates, with the chemical composition presented in Table 1. The electrolyte was a 3.5 wt.% NaCl solution consisting of analytical grade NaCl supplied by Merck dissolved in distilled water. Zinc aluminum polyphosphate (ZAPP), supplied by Heubach Ltd. was used as anticorrosion pigment (chemical composition and property data sheet presented in Table 2). The organic inhibitor was 2-mercaptobenzimidazole (MBI) purchased from Merck with the chemical structure illustrated in Fig. 1. The epoxy resin was based on bisphenol-A (SL 75 × 4171) purchased from Jubail Chemical Industries Co. (JANA). The epoxy resin solid content, value and density were 74–76%, 1.49–1.67 Eq/kg, and 1.08 g cm^{-3}, respectively. The epoxy hardener was amino polyamide, CRAYAMID 115, purchased from Arkema Co. The solid content, density and viscosity values of the hardener were 50%, 0.97 g/cm^3 and 50,000 cps, respectively at 40 °C. The epoxy solvent was a mixture of Butyl glycol, Toluene and Methyl ethyl ketone supplied by Merck.

2.2. Solution phase study

To study the effect of ZAPP on the steel corrosion as an inorganic inhibitor, the pigment extract, 2 g of ZAPP was stirred in 1.0 l 3.5 wt.% NaCl solution for 24 h and filtered to obtain the saturation condition [22]. In the case of MBI, organic inhibitor, the solution was composed of 0.86 mM of MBI in 3.5 wt.% NaCl solution [16]. Since MBI is only slightly soluble in water and completely soluble in ethanol, it was dissolved in ethanol initially and subsequently added to the aqueous electrolyte solution. To prepare the MBI-ZAPP mixture, 0.86 mM of MBI was added to the pigment extract solution. The pH value of all the prepared solutions was in the range of 6.5 and 7.0.

The electrochemical evaluation of inhibitors was performed using a Gill AC potentiostat (ACM instrument) with a conventional three electrode cell. The working electrode was a cold-mounted mild steel rod with 1 cm^2 active area, while a saturated calomel electrode (SCE) and a platinum wire were employed as the reference and the counter electrode, respectively. After immersion of the bare steel into the solutions for 1 h, linear polarization resistance (LPR) tests were performed from −15 to +15 mV versus OCP at a sweep rate of 10 mV/min up to 24 h. The LPR values were calculated using current-potential plots where the slopes become linear. In addition, potentiodynamic polarization curves were recorded from −250 to +250 mV versus OCP at a scan rate of 30 mV/min, after 24 h immersion. To explore the anodic dissolution

Table 2
Chemical composition and property datasheet of the ZAPP pigment.

Trademark	Zn (%)	Phosphorus as P$_2$O$_5$ (%)	Al (%)	Density (g/cm^3)	Average particle size (μm)	Loss on ignition 600 °C
HEUCOPHOS ZAPP	28–31	46–49	11–13	3.1	2–3.5	8–12
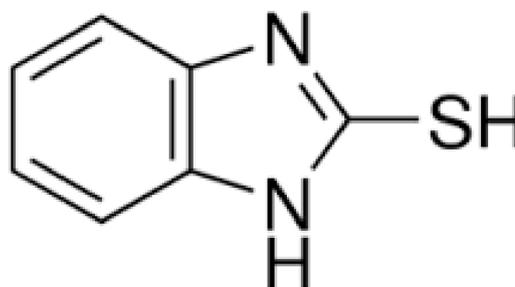
Fig. 1. Molecular structure of 2-mercaptobenzimidazole (MBI).

behavior of mild steel in 3.5 wt.% NaCl solution containing 0.86 mM MBI, potentiostatic polarization tests were performed at -600 and −450 mV vs. SCE and the corresponding current densities were recorded for 20 min. A 500 ml beaker, open to the air, was used as the electrochemical cell.

SEM studies using a FEI Helios G4 microscope were carried out to study the morphology of the layer formed on the steel surface after 96 h of immersion in the solutions. To chemically evaluate the surfaces exposed to the solutions, a Thermo-nicolet Nexus FTIR apparatus was used equipped with a mercury-3 cadmium-telluride liquid-nitrogen cooled detector and a nitrogen-purged measurement chamber. The FTIR measurements were conducted by reflection of the incident beam at an angle of incidence of 80° using p-polarized radiation. The measurements were conducted versus backgrounds collected before the exposures.

2.3. Coating preparation and evaluation

Blank coatings were prepared with no pigment and inhibitor to be used as Reference. 7 wt.% Butyl glycol, 75 wt.% Toluene and 18 wt.% Methyl ethyl ketone (epoxy solvent) were mixed by the epoxy binder to reach a viscosity of 85 cps at 25 °C. Afterward, 25 wt.% polyamide hardener was added to 75 wt.% epoxy, followed by a mixing step using a high speed mechanical stirrer until a homogenous mixture was obtained.

The epoxy coating with MBI (MBI + epoxy coating) was prepared by adding 1.5 g of MBI to 100 g of epoxy coating. At first stage, MBI was added to the hardener and the amount of hardener was calculated to reach the stoichiometry ratio of 75/25 epoxy /hardener. In order to adjust the intended viscosity, i.e. 85 centipoises, the solvent was added to epoxy, followed by mixing the blend using a high speed mechanical stirrer and milling to the particle size of approximately 10 μm.

Besides, ZAPP was incorporated into the epoxy (ZAPP + epoxy coating) to study its effect as a leaching inorganic inhibitor. The effective ratio of the pigment volume concentration (PVC) to the critical pigment volume concentration (CPVC) is λ = PVC/CPVC = 0.6 reported by Naderi and Attar [22]. Thus, 47.4 g of ZAPP anticorrosion pigment was added to the epoxy resin to prepare 100 g coating. Additionally, 4.1 g of Bentone 34 and 1 g of dispersing agent (NUOSPERSE 657) were added to improve the film formation. The obtained blend was ball milled for 24 h to obtain a homogenous mixture with a particle size smaller than 15 μm. Afterward, the mixture viscosity was adjusted using the solvent and hardener added to the mixture. Finally, the obtained mixture was mechanically stirred to obtain a homogenous mixture.

Finally, a group of coatings was prepared by incorporating ZAPP and MBI into the epoxy. The first preparation stage of ZAPP + MBI + epoxy was the same as ZAPP + epoxy coating, although the ZAPP value was 45.9 g. After a 24-h ball milling and addition of 1.5 g of MBI, the blend was mixed with a high-speed disk disperser for 10 min. The sum of MBI and ZAPP value was 47.4 g in order to attain a λ value of 0.6. To reach the intended viscosity, the solvent was added to the blend and the final mixture was mechanically stirred after adding

the hardener.

Prior to application of the coatings, the steel plates were cleaned in acetone followed by pickling process in 20 wt.% hydrochloric acid solutions for 10 min [30]. The prepared coatings were applied on the steel plates using a film applicator. The coated samples were cured in an oven set at 80 °C for 40 min and subsequently stored for 7 days at room temperature [31]. The dry film thicknesses were estimated to be 46 ± 5 μm using an optical microscope. To perform electrochemical tests, the coated samples were sealed with a mixture of beeswax and colophony resin, leaving a central area of 15 cm² unmasked. From each coating group, three samples were prepared to confirm reproducibility of the electrochemical and adhesion strength tests.

EIS measurements were carried out on the intact coatings using an Ivium potentiostat in the frequency range of 100 kHz to 0.01 Hz, and AC signal with an amplitude of 10 mV around open circuit potential (OCP) for a duration of 70 days. All measurements were repeated at least 3 times to check the reproducibility of the results. The electrochemical cell was a 500 ml beaker which was open to the air.

Adhesion strengths of the coatings were determined by a direct pull-off standard procedure (ASTM D 4541) using a Positest-AT digital Pull-off adhesion tester. The adhesion measurements were performed prior to the immersion in 3.5 wt.% NaCl solution (dry adhesion) and after 60 days of immersion in 3.5 wt% NaCl solution at room temperature (wet adhesion). An epoxy adhesive (OHO) was employed to perform the pull-off test. After 72 h curing of the OHO adhesive at room temperature, the coatings were cut around the dolly, while the dolly was pulled off perpendicular to the surface. For each type of the coating, 3 samples were examined and minimum forces to detach the coatings from the substrates (adhesive failure) were recorded.

3. Results

3.1. Solution phase study

3.1.1. Electrochemical evaluations

The intrinsic inhibition performances of MBI, ZAPP and the MBI-ZAPP mixture for the steel substrates are studied electrochemically in the 3.5 wt.% NaCl solution. The system under study is complex enough, not allowing the corrosion current to be estimated via simple LPR or Tafel extrapolation methods. Nevertheless, the efficiency of the inhibitors via LPR can be explored by assuming that there is a correlation between the polarization resistance (zero frequency limit in the impedance diagrams) and the corrosion rate [32]. In fact, such a measured resistance value is not exactly the resistance of polarization, but it can be employed to evaluate the relative effectiveness of each inhibitor used later in the epoxy system. Fig. 2 shows the LPR values of the bare steel substrates immersed in the solutions up to 24 h. It can be seen that MBI exhibits no significant effect over the 24 h immersion and shows similar polarization resistance values to those of the blank sample (approx. 1 kΩcm²). ZAPP moderately increases the polarization resistance, while the LPR values increase from 12 kΩcm² to 22 kΩcm² after 12 h followed by a slight decrease to 20 kΩcm² in 12–24 h. However, the mixed inhibitors show a remarkable impact on the LPR values rising steadily from 12 to 50 kΩcm² within the initial 18 h followed by a slight drop of 3 kΩcm² in the 18–24 h exposure timeframe.

Fig. 3 shows the electrochemical polarization curves collected to further evaluate the inhibitor performances. It can be seen that ZAPP diminishes both anodic and cathodic current densities, while a reduction of the anodic current density is more pronounced. The results also show that the MBI-ZAPP mixture significantly decreases both anodic and cathodic currents verifying the LPR results indicating the significant effect of the mixed system. On the other hand, MBI slightly reduces the cathodic current density, whereas the anodic current density is increased at potentials higher than −560 mV vs. SCE indicating accelerated corrosion at anodic potentials. This phenomenon is further explored by running potentiostatic polarization measurements on the
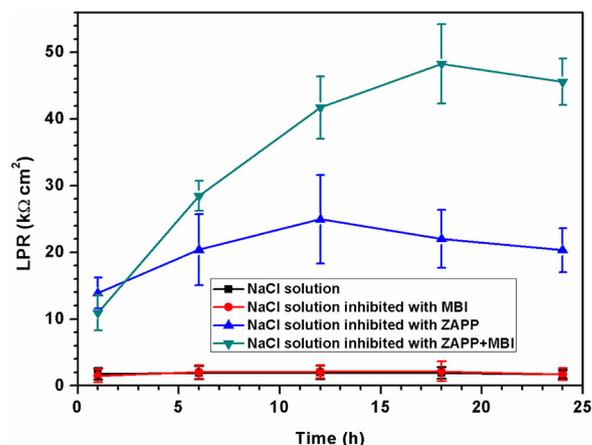

Fig. 2. Linear polarization resistance of the steel during the 24 h immersion in various solutions. The solutions are 3.5 wt.% NaCl, 3.5 wt.% NaCl + 0.86 mM MBI, 3.5 wt.% NaCl + ZAPP extract and 3.5 wt.% NaCl + 0.86 mM MBI + ZAPP extract. The error bars show the standard deviation for 3 identical samples.
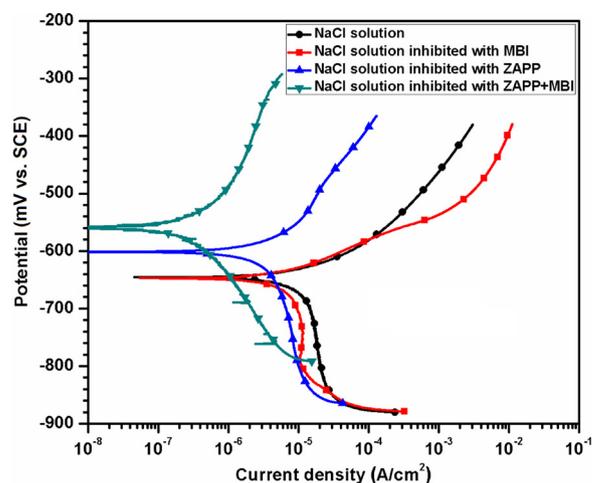

Fig. 3. Polarization curves of mild steel in different solutions after 24 h immersion. The solutions are 3.5 wt.% NaCl, 3.5 wt.% NaCl + 0.86 mM MBI, 3.5 wt.% NaCl + ZAPP extract and 3.5 wt.% NaCl + 0.86 mM MBI + ZAPP extract.
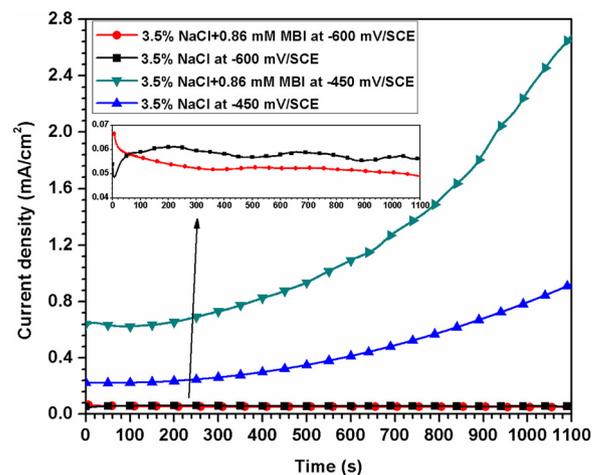

Fig. 4. Anodic current density of mild steel in the blank and MBI inhibitor-containing solution. The curves are recorded during a potentiostatic polarization of the samples at −600 and −450 mV vs. SCE for approximately 20 min. Prior to the potentiostatic test, a stabilization period of 1 h was implemented.
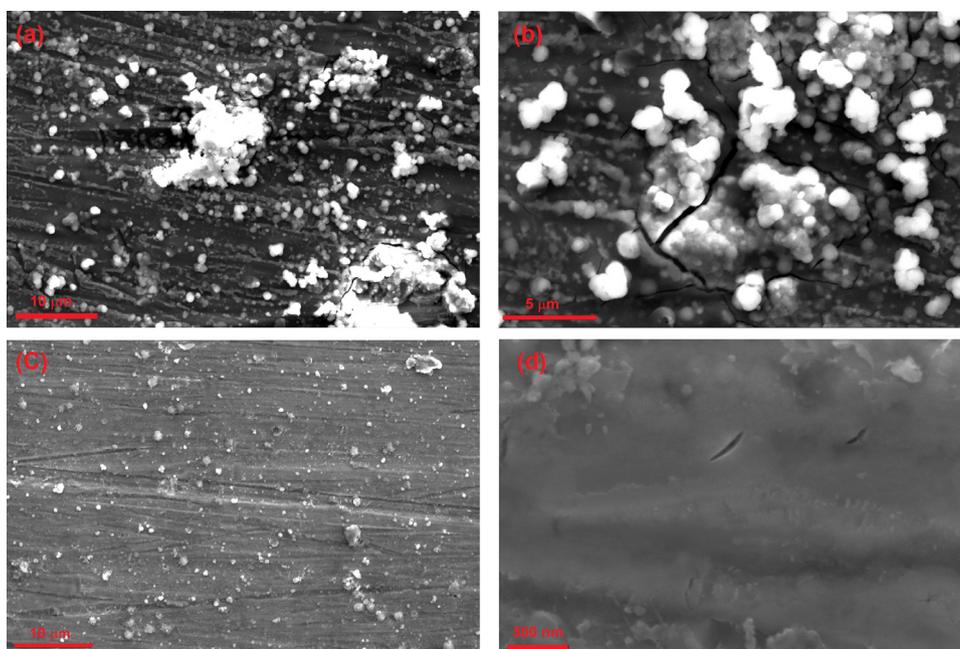
Fig. 5. SEM images of the steel surface exposed to the NaCl solution containing (a and b) ZAPP and (c and d) ZAPP + MBI.

blank and MBI-containing solutions at −600 and −450 mV vs. SCE as shown in Fig. 4. These potentials are selected to evaluate the current densities around the observed critical potential, i.e. −560 mV vs. SCE. It can be seen that MBI slightly lowers the current density at −600 mV vs. SCE as compared to the blank solution whereas the current density is increased at −450 mV vs. SCE for the inhibitor-containing solution than that of the blank one indicating a higher dissolution rate.

3.1.2. Surface analysis

The SEM images of the steel exposed to the NaCl solution containing ZAPP and ZAPP + MBI after 96 h were presented in Fig. 5. Comparison of Fig. 5(a) and (c) shows that a larger amount of corrosion products has been formed on the surface immersed in ZAPP solution. A closer look (Fig. 5(b)) reveals that the corrosion products are accumulated around the microcracks of the ZAPP layer. Although the artefacts are observed also on the layer formed by a mixture of ZAPP and MBI (Fig. 5(d)), the ZAPP layer indeed contains numerous larger cracks.

Fig. 6 shows FTIR spectra of MBI and ZAPP samples collected versus the bare steel background, and the spectrum of MBI + ZAPP samples collected versus the ZAPP background. The later spectrum was collected versus ZAPP background to subtract the ZAPP peaks and identify additional functional groups incorporated in the deposited layer due to the presence of MBI. Spectrum (a) exhibits a week peak around 1100 cm^{-1} presumably originating from the metal oxide whereas the C−H and C−N peaks expected from the MBI functional groups are missing. On the other hand, the FTIR spectrum of ZAPP collected versus the steel substrate (Spectrum (b)) shows a broad and intense peak around 1100 cm^{-1} indicating the presence of P−O and P=O compounds on the surface which in turn reveals formation of ZAPP-incorporating layer on the steel surface. Additionally, Spectrum (c) shows clear peaks at 748, 1086, 1222, 1268, 1291, 1380 and 1429 cm^{-1} which originate from the MBI compound as the ZAPP vibrational bands are excluded from the background [33–35].

3.2. Corrosion inhibition of the coated substrates

The electrochemical studies showed that a mixture of the inhibitors enhances the corrosion resistance of the steel substrates exposed to the corrosive solution. In this section, we aim to evaluate behaviors of the MBI, ZAPP and a MBI-ZAPP mixed inhibitors incorporated in an epoxy-
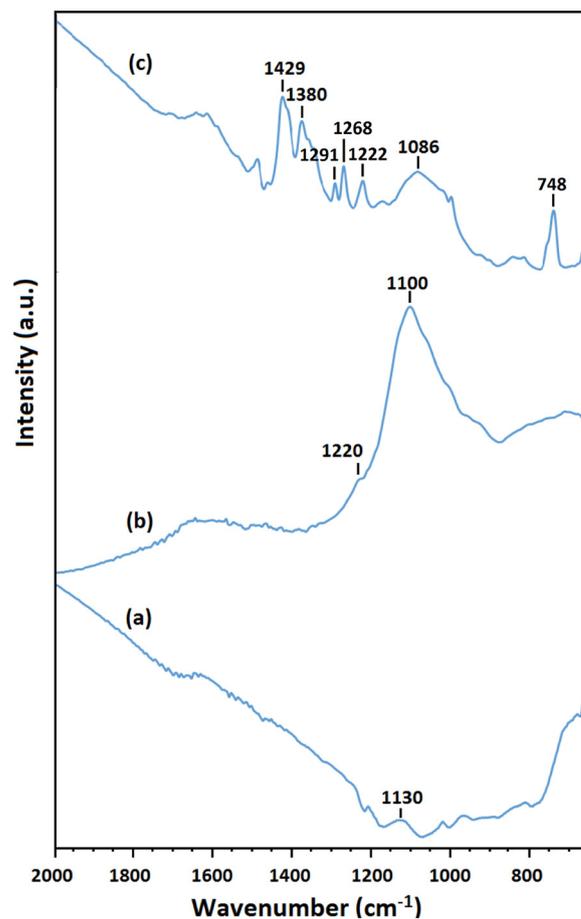

Fig. 6. FTIR spectra acquired from the samples exposed to 3.5 wt.% NaCl solution containing (a) MBI, (b) ZAPP and (c) a mixture of MBI and ZAPP.

polyamide coating system.

3.2.1. Long term OCP recording

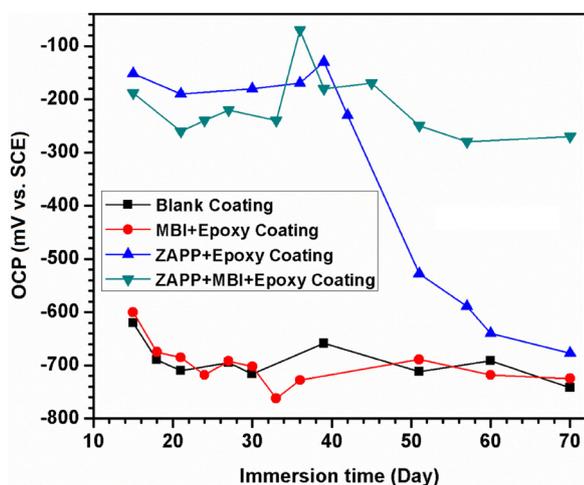Fig. 7 shows OCP variations of the coated undoped samples (blank)

Fig. 7. OCP evolution of the coated mild steel substrates during immersion in 3.5 wt.% NaCl solution up to 70 days.

and those doped with MBI, ZAPP and ZAPP + MBI for 70 days of immersion in 3.5 wt.% NaCl solutions. Each data point in the graph is an average of three measurements. It can be seen that the OCP values of the blank and MBI + epoxy coated samples remain relatively constant over the immersion period. Their OCPs are initially around −600 mV vs. SCE and decrease gradually to −700 mV vs. SCE within 20 days and remain almost unchanged until the end of exposure. The ZAPP + epoxy sample presents an OCP value of ∼ −150 mV vs. SCE during the initial 40 days followed by a gradual drop to −700 mV vs. SCE. The OCP of the ZAPP + MBI + epoxy coated sample starts from −150 mV vs. SCE and remains relatively constant over the exposure period.

3.2.2. Long term impedance measurements

EIS measurements were conducted in order to assess the durability of the coatings in 3.5 wt.% NaCl solution. Fig. 8 shows the Bode and phase plots of the blank, MBI + epoxy, ZAPP + epoxy and ZAPP + MBI + epoxy coated samples after 70 days. The Bode plots show different impedance values for the samples, indicating dissimilar electrochemical behavior. Besides, the phase plots of all the coated systems clearly show two distinct time constants, except for the ZAPP + MBI + epoxy coated sample which reveals a plateau-like behavior from the high to relatively low frequency range. It is reported by Mansfeld [3] that the phase plot of the coated system exhibits such a behavior when the organic coating has undergone little degradation. Thus, in order to quantitatively analyze the impedance spectra, the experimental data were fitted to an electrical equivalent circuit representing an electrode coated with a porous layer as shown in Fig. 8(a) [36]. In this model, the time constant at high frequencies is related to the coating pores and another one at low frequencies is correlated to the polarization resistance of the steel substrate [37–40]. The representative model consists of an electrolyte resistance (R_s), coating capacitance (C_c) and pore resistance (R_c). Additionally, the constant phase element (CPE_{dl}) represents the double layer capacitance parallel with a metal polarization resistance (R_p). The CPE element is a non-ideal capacitance widely used to model the imperfect dielectric behavior [36]. The CPE value can be calculated using Eq. (1):

$$CPE_{dl} = P^{1/n} R_P^{1-n/n} \tag{1}$$

where P is the magnitude of CPE and n the deviation parameter [41]. The corresponding fitted lines of the Nyquist and Bode plots of the coated samples after 70 days of immersion are shown in Fig. 8 indicating good fittings with the proposed model. The resistance and capacitance values are extracted from the fittings providing quantitative information about the electrochemical phenomena and
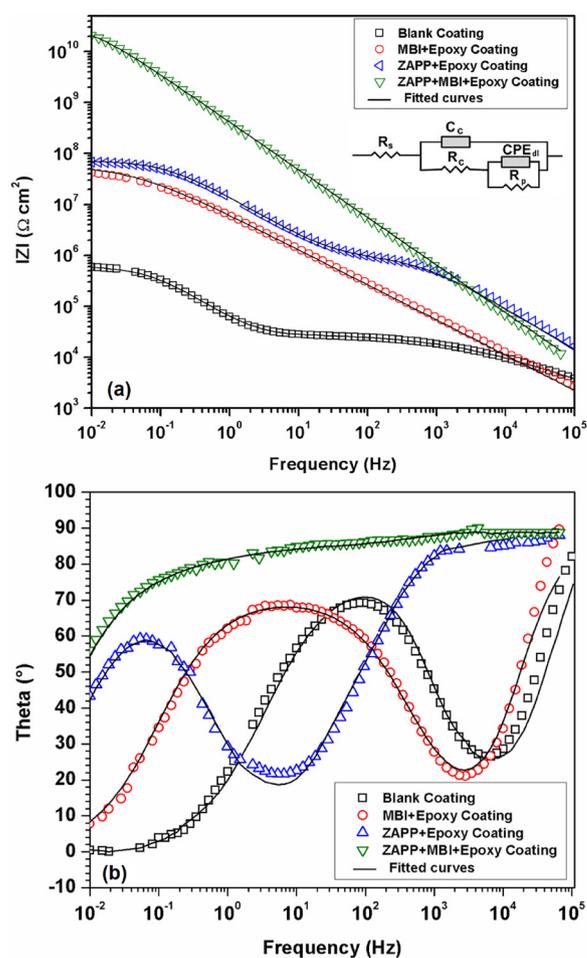

Fig. 8. (a) Bode and (b) phase plots of the coatings after 70 days of immersion in 3.5 wt.% NaCl solution. The equivalent circuit model is used to fit the EIS results.

degradation processes of the coated samples. Fig. 9(a) shows the EIS, polarization resistance (R_p) of different samples as a function of the immersion time. R_p of the blank coated sample decreases steadily from 10^2 to 1 MΩcm^2 over the exposure time. The MBI + epoxy coated sample shows a slight increase of the R_p value within 20 days followed by a sharp decrease to 10 MΩcm^2 and a consequent R_p drop to slightly higher values than the blank sample after 70 days of exposure. During the initial 30 days of the immersion, ZAPP + epoxy and ZAPP + MBI + epoxy coated samples present relatively similar and constant R_p values, i.e. ∼ 5.10^4 MΩcm^2. Afterward, the ZAPP + MBI + epoxy coated sample shows a stable R_p value, however, the ZAPP + epoxy sample shows a gradual drop by two orders of magnitudes up until 40 days followed by relatively constant R_p values towards the end of exposure.

Fig. 9(b) shows the double layer capacitance (C_{dl}) values of the coated samples over the 70 days of immersion. Among the samples, MBI + ZAPP + epoxy coating exhibits the lowest double layer capacitance (C_{dl}), i.e. ∼0.5 nF cm^2, which remains relatively constant throughout the exposure period. All the inhibitor-containing coated samples show similar C_{dl} values in the beginning of the exposure, whereas the C_{dl} values of the MBI + epoxy and ZAPP + epoxy coated samples show a dramatic rise to 10 and 100 nF.com^2 after respectively 20 and 30 days. On the other hand, the blank coating shows an initial rise and a consequent drop of the C_{dl} values within 20 days where a linear increase is exhibited at 10 days onwards.

Fig. 10(a) shows pore resistance (R_c) variations during 70 days of immersion in the NaCl solution. R_c values of the blank coating exhibit
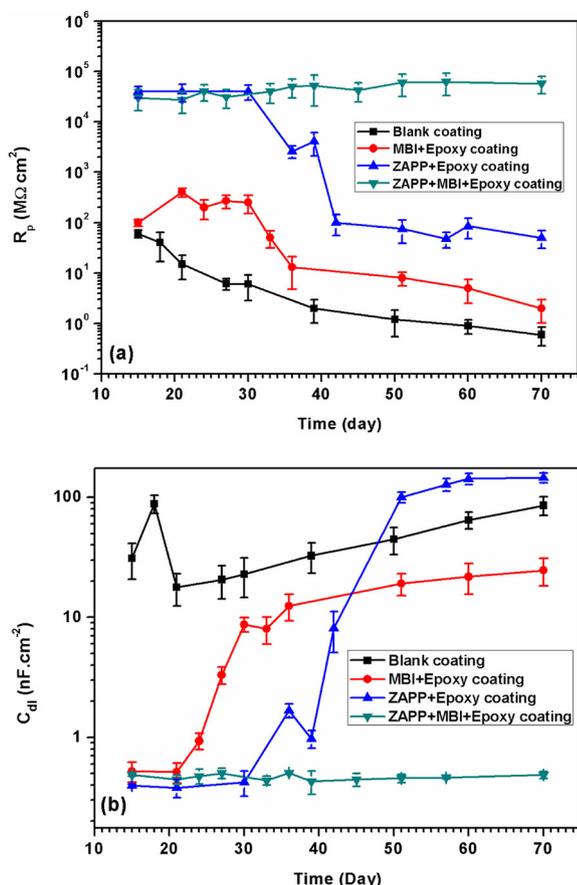
Fig. 9. Polarization resistance (a) and double layer capacitance (b) of different coatings versus exposure time.

fluctuations during the initial 20 days followed by a sudden decrease of two orders of magnitude. The MBI + epoxy coated sample experiences a similar trend, whereas the initial R_c value is higher than that of the blank one. The ZAPP + epoxy coated sample shows much higher R_c values, and the MBI + ZAPP + epoxy coating exhibits the highest R_c values among the samples studied. In fact, steel samples coated with ZAPP + epoxy and MBI + ZAPP + epoxy show equal R_c values within the initial 40 days, whereas ZAPP + epoxy experiences a steep R_c drop of one order of magnitude after 40 days. Fig. 10(b) demonstrates the C_c values over 70 days of immersion. The ZAPP + MBI + epoxy coated sample presents the lowest and the most stable C_c values among the coatings studied over the immersion period. In contrast, C_c values of the other coatings rise with exposure time, where the blank coating shows the highest C_c values among the samples.

3.2.3. Adhesion properties

Fig. 11 shows the pull-off test results conducted in dry and wet conditions. Overall, all coatings exhibit similar initial adhesion strengths where there is ~ 0.25 MPa difference between the highest and lowest values. However, the exposed samples show different adhesion strength values. The adhesion strength of the blank coating is equal to 0.9 MPa under dry conditions and 0.4 MPa in wet conditions. MBI + epoxy coating shows slightly higher adhesion strengths, i.e. 1 MPa in dry and 0.5 MPa in wet condition. The ZAPP + epoxy coating shows a dry adhesion strength of 1.2 MPa and wet adhesion strength of 0.9 MPa. MBI + ZAPP + epoxy coating shows a dry adhesion strength of 1.1 MPa which dropped to 1.0 MPa after 60 days.
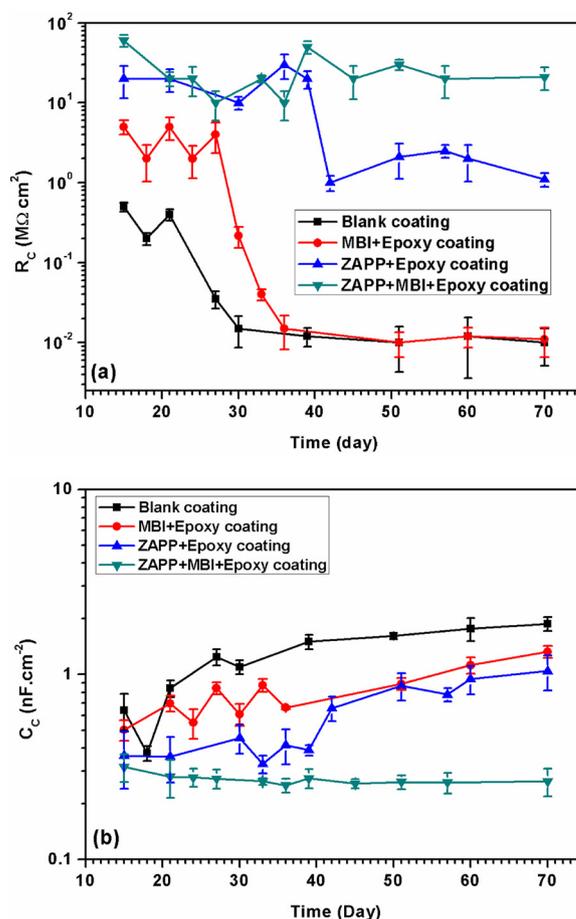
Fig. 10. Coating resistance (a) and coating capacitance (b) values of different coatings versus exposure time.
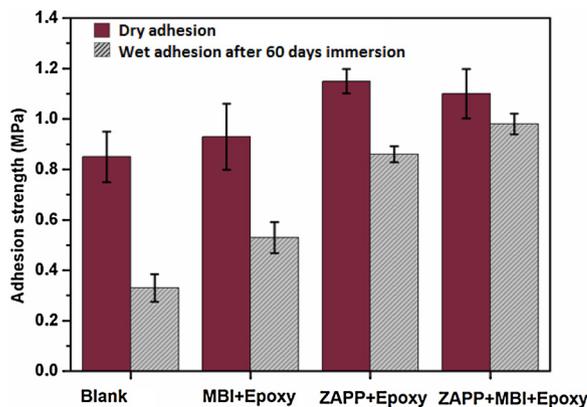
Fig. 11. Adhesion strength of the coated samples under dry conditions and after 60 days of immersion in 3.5 wt.% NaCl solution (wet condition).

4. Discussion

4.1. Inhibitor-metal interactions

MBI is recognized as a good inhibitor for steel substrates in acidic media where iron oxides are unstable [28]. However, FTIR showed that MBI has a weak interaction with the steel substrate in the NaCl solution presumably due to the presence of oxides. The potentiodynamic and potentiostatic polarization measurements indicated that the MBI interaction to the steel surfaces is potential-dependent where it becomes a weak corrosion inhibitor at cathodic potentials and a corrosion

accelerator at anodic potentials. Therefore, it may be interpreted that although MBI interacts with the steel surfaces through physisorption, it can accelerate the anodic dissolution at noble potentials possibly because of the modification of the anodic dissolution process [42].

ZAPP is expected to establish a protective layer, composed of zinc hydroxide/phosphate and iron phosphate, through a precipitation process [43]. The layer decreases both anodic and cathodic current densities of the steel substrates in 3.5 wt.% NaCl indicating barrier properties of the formed layer. Phosphates of the ZAPP structure can strongly interact with the oxide layers through an acid and base interaction [42]. A mixture of the MBI and ZAPP inhibitors exhibited a substantial corrosion inhibition improvement as compared to solely MBI and ZAPP-containing solutions indicated by the electrochemical measurements. The SEM images reveal that the layer formed by ZAPP + MBI contains less cracks, providing a more protective layer which effectively hinders corrosion. The FTIR studies show that MBI is incorporated in the protective layer formed on the steel surface when the mixed system was used, whereas MBI is hardly detected on the steel surface when MBI was not mixed with ZAPP. Therefore, it can be interpreted that ZAPP provides the nucleation sites for incorporation of MBI in the protective layer. ZAPP may initially precipitate functionalizing the steel surface for adsorption of MBI. This process can be fulfilled through the electrostatic interaction of lone electron pairs of N and S in the molecular structure of MBI with vacant orbitals of Zn and Al in ZAPP [44]. Therefore, MBI can play the role of reinforcing agent so that the ZAPP layer in the presence of MBI contains smaller and lesser cracks. As schematically shown in Fig. 12, the electrolyte can easily reach the steel substrate through larger cracks of the ZAPP layer (Fig. 12(a)) whereas the synergetic effect of ZAPP and MBI leads to the formation of a robust layer with lower defects, leading to efficiently inhibiting the steel corrosion and consequently minor corrosion products (Fig. 12(b)).

4.2. Inhibitor-incorporated coatings

According to the results, the sample coated with MBI + epoxy shows a slightly improved corrosion resistance, compared to the blank coated sample. Incorporation of ZAPP in the epoxy coating makes the steel substrate moderately corrosion resistant, while the mixed ZAPP and MBI system substantially improves the corrosion resistance. The enhanced corrosion protection of the mixed system incorporated in the polymer coating indicates that both inhibitors can efficiently leach out and also cooperatively establish a protective layer on the steel surface. The composition of the protective layer formed due to the incorporated inhibitors in the polymer coating may deviate from that of those formed in solution as the electrolyte compositions are expected to be different within/under the coatings and in the solution [13].

The OCP values show that there is an active corrosion underneath the blank and MBI + epoxy coatings while the OCP values for the ZAPP + epoxy and ZAPP + MBI + epoxy coated mild steel surface remains at noble potentials. However, the most durable passivity for the steel is obtained for the ZAPP + epoxy coating. R_p values represent both charge transfer and resistivity of the deposited layer indicating the protection quality of the deposited layer at the metal/coating interface.

Therefore, the leached-out MBI hardly protects the steel substrate against corrosion, whereas an improved protection is detected for ZAPP during the initial exposure time only. The gradual R_p decrease of ZAPP over the exposure time indicates a lack of integrity of the layer formed. On the other hand, the enhanced corrosion protection detected for the mixed MBI and ZAPP system remains constant over the entire exposure time indicating formation of a robust and durable layer at the metal/coating interface.

An increase of the active area gives rise to an increase of the double layer capacitance (C_{dl}) value. Therefore, the C_{dl} value increase indicates corrosion propagation at the metal/coating interface. The Helmholtz model relates the capacitance value to the structural parameters as follows [45]:

$$C = \frac{\varepsilon^0 \varepsilon}{d} S \qquad (2)$$

where d is the coating thickness, S the electrode surface, ε° the permittivity of air and ε the local dielectric constant. The large C_{dl} values of the samples with the blank and MBI coatings indicate that corrosion takes place on steel surfaces resulting in formation of porous corrosion products easily soaked with electrolyte possessing a high dielectric constant. Therefore, it can be inferred that these two coatings do not establish any protective layer. The samples coated with ZAPP + epoxy and MBI + ZAPP + epoxy coatings present lower C_{dl} values indicating formation of protective layers against water diffusion and corrosion propagation. However, ZAPP + epoxy sample loses the integrity with immersion time.

The initial R_c values show that the samples coated with the blank and MBI + epoxy coatings exhibit higher amounts of pores or capillary channels in comparison with the other two coatings. Thus, the electrolyte can easily reach the surface through these defects [46]. Owing the fact that the coating delamination results in a decrease of the R_c values, corrosion propagates beneath the blank and MBI + epoxy coatings [38,46]. Although both ZAPP + epoxy and MBI + ZAPP + epoxy coatings retard delamination by releasing the inhibitors, the latter shows a more durable corrosion protection. The surface area and local dielectric constant variations promoted respectively by delamination and water uptake is responsible for the coating capacitance (C_c) changes [3,46,47]. Thus, a protective layer hinders corrosion which is particularly the case for the MBI + ZAPP + epoxy coated sample. This fact can surely enhance the adhesion properties, as confirmed by the adhesion tests in which the ZAPP + MBI coating shows a remarkable remaining wet adhesion strength after 60 days among the coatings studied.

5. Conclusions

This study evaluates the performance of epoxy-polyamide coatings doped with zinc aluminum polyphosphate (ZAPP) and 2-mercapto-benzimidazole (MBI) inhibitors immersed in 3.5 wt.% NaCl solution for 70 days. It was found that the steel substrate coated with MBI + ZAPP shows a remarkable and durable corrosion resistance during the immersion. This is correlated to the leached-out inhibitors forming a robust layer at the metal/coating interface. It was shown that MBI-only
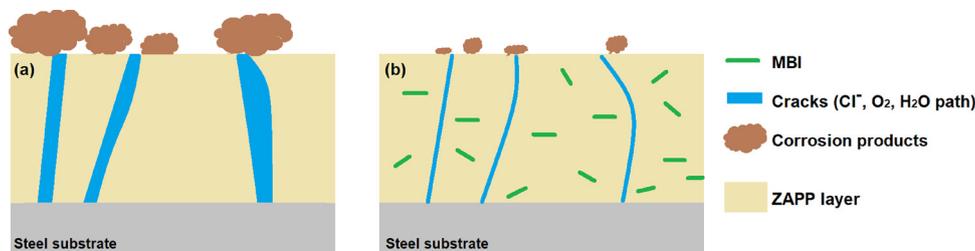

Fig. 12. Schematic representation of the formation mechanism of the protective layer formed in the NaCl solution containing (a) ZAPP and (b) ZAPP + MBI.

lacks the capacity to form a robust and protective layer at the metal/coating interface, whereas a mixed MBI and ZAPP system cooperatively establishes a protective layer composed of both inhibitors. Since MBI has no strong interaction with the steel surface, it turns out that ZAPP forms nucleation sites for adsorption of MBI which reinforces the ZAPP layer, promoting a dense layer that contains less defects.

Data availability

The raw/processed data required to reproduce these findings cannot be shared at this time due to technical or time limitations.

Acknowledgments

References

[1] G. Grundmeier, W. Schmidt, M. Stratmann, Corrosion protection by organic coatings: electrochemical mechanism and novel methods of investigation, Electrochim. Acta 45 (2000) 2515–2533.

[2] S. Haruyama, M. Asari, T. Tsuru, Corrosion protection by organic coatings, Electrochem. Soc. Proc. 87–2 (1987) 197.

[3] F. Mansfeld, Use of electrochemical impedance spectroscopy for the study of corrosion protection by polymer coatings, J. Appl. Electrochem. 25 (1995) 187–202.

[4] T. Chou, C. Chandrasekaran, S. Limmer, S. Seraji, Y. Wu, M. Forbess, C. Nguyen, G. Cao, Organic–inorganic hybrid coatings for corrosion protection, J. Non-Cryst. Solids 290 (2001) 153–162.

[5] D. Raps, T. Hack, J. Wehr, M. Zheludkevich, A. Bastos, M. Ferreira, O. Nuyken, Electrochemical study of inhibitor-containing organic–inorganic hybrid coatings on AA2024, Corros. Sci. 51 (2009) 1012–1021.

[6] M.G. Sari, B. Ramezanzadeh, M. Shahbazi, A.S. Pakdel, Influence of nanoclay particles modification by polyester-amide hyperbranched polymer on the corrosion protective performance of the epoxy nanocomposite, Corros. Sci. 92 (2015) 162–172.

[7] B. Ramezanzadeh, S. Niroumandrad, A. Ahmadi, M. Mahdavian, M.M. Moghadam, Enhancement of barrier and corrosion protection performance of an epoxy coating through wet transfer of amino functionalized graphene oxide, Corros. Sci. 103 (2016) 283–304.

[8] N. Pirhady Tavandashti, M. Ghorbani, A. Shojaei, J.M.C. Mol, H. Terryn, K. Baert, Y. Gonzalez-Garcia, Inhibitor-loaded conducting polymer capsules for active corrosion protection of coating defects, Corros. Sci. 112 (2016) 138–149.

[9] A. Yabuki, T. Shiraiwa, I.W. Fathona, pH-controlled self-healing polymer coatings with cellulose nanofibers providing an effective release of corrosion inhibitor, Corros. Sci. 103 (2016) 117–123.

[10] S. Pour-Ali, C. Dehghanian, A. Kosari, In situ synthesis of poly-aniline–camphorsulfonate particles in an epoxy matrix for corrosion protection of mild steel in NaCl solution, Corros. Sci. 85 (2014) 204–214.

[11] G. Gupta, N. Birbilis, A. Cook, A. Khanna, Polyaniline-lignosulfonate/epoxy coating for corrosion protection of AA2024-T3, Corros. Sci. 67 (2013) 256–267.

[12] M. Saremi, M. Yeganeh, Application of mesoporous silica nanocontainers as smart host of corrosion inhibitor in polypyrrole coatings, Corros. Sci. 86 (2014) 159–170.

[13] D. Snihirova, S.V. Lamaka, P. Taheri, J.M.C. Mol, M.F. Montemor, Comparison of the synergistic effects of inhibitor mixtures tailored for enhanced corrosion protection of bare and coated AA2024-T3, Surf. Coat. Technol. 303 (2016) 342–351 Part B.

[14] A. Thorn, A. Adam, T. Gichuhi, W. Novelli, M.A. Sapp, Improved corrosion control through nontoxic corrosion inhibitor synergies, JCT Coat. Technol. 3 (2006) 24–30.

[15] N. Birbilis, R. Buchheit, D. Ho, M. Forsyth, Inhibition of AA2024-T3 on a phase-by-phase basis using an environmentally benign inhibitor, cerium dibutyl phosphate, Electrochem. Solid-State Lett. 8 (2005) C180–C183.

[16] M.S. Ghaffari, R. Naderi, M. Sayehbani, The effect of mixture of mercaptobenzimidazole and zinc phosphate on the corrosion protection of epoxy/polyamide coating, Prog. Org. Coat. 86 (2015) 117–124.

[17] J. Mardel, S.J. Garcia, P.A. Corrigan, T. Markley, A.E. Hughes, T.H. Muster, D. Lau, T.G. Harvey, A.M. Glenn, P.A. White, S.G. Hardin, C. Luo, X. Zhou, G.E. Thompson, J.M.C. Mol, The characterisation and performance of Ce(dbp)3-inhibited epoxy coatings, Prog. Org. Coat. 70 (2011) 91–101.

[18] S. Kallip, A.C. Bastos, K.A. Yasakau, M.L. Zheludkevich, M.G. Ferreira, Synergistic corrosion inhibition on galvanically coupled metallic materials, Electrochem. Commun. 20 (2012) 101–104.

[19] M. Mahdavian, S. Ashhari, Mercapto functional azole compounds as organic corrosion inhibitors in a polyester-melamine coating, Prog. Org. Coat. 68 (2010) 259–264.

[20] A. Balaskas, I. Kartsonakis, D. Snihirova, M. Montemor, G. Kordas, Improving the corrosion protection properties of organically modified silicate–epoxy coatings by incorporation of organic and inorganic inhibitors, Prog. Org. Coat. 72 (2011) 653–662.

[21] H.R. Asemani, P. Ahmadi, A.A. Sarabi, H. Eivaz Mohammadloo, Effect of zirconium conversion coating: adhesion and anti-corrosion properties of epoxy organic coating containing zinc aluminum polyphosphate (ZAPP) pigment on carbon mild steel, Prog. Org. Coat. 94 (2016) 18–27.

[22] R. Naderi, M. Attar, Electrochemical study of protective behavior of organic coating pigmented with zinc aluminum polyphosphate as a modified zinc phosphate at different pigment volume concentrations, Prog. Org. Coat. 66 (2009) 314–320.

[23] B. Del Amo, R. Romagnoli, V. Vetere, L. Hernández, Study of the anticorrosive properties of zinc phosphate in vinyl paints, Prog. Org. Coat. 33 (1998) 28–35.

[24] A. Kalendova, D. Veselý, J. Brodinova, Anticorrosive spinel-type pigments of the mixed metal oxides compared to metal polyphosphates, Anti-Corros. Method M 51 (2004) 6–17.

[25] J. Aljourani, K. Raeissi, M. Golozar, Benzimidazole and its derivatives as corrosion inhibitors for mild steel in 1M HCl solution, Corros. Sci. 51 (2009) 1836–1843.

[26] H. Amar, A. Tounsi, A. Makayssi, A. Derja, J. Benzakour, A. Outzourhit, Corrosion inhibition of Armco iron by 2-mercaptobenzimidazole in sodium chloride 3% media, Corros. Sci. 49 (2007) 2936–2945.

[27] M. Finšgar, 2-Mercaptobenzimidazole as a copper corrosion inhibitor: Part I. Long-term immersion, 3D-profilometry, and electrochemistry, Corros. Sci. 72 (2013) 82–89.

[28] M. Mahdavian, S. Ashhari, Corrosion inhibition performance of 2-mercaptobenzimidazole and 2-mercaptobenzoxazole compounds for protection of mild steel in hydrochloric acid solution, Electrochim. Acta 55 (2010) 1720–1724.

[29] L. Wang, J.-X. Pu, H.-C. Luo, Corrosion inhibition of zinc in phosphoric acid solution by 2-mercaptobenzimidazole, Corros. Sci. 45 (2003) 677–683.

[30] Y. Liu, L. Wang, L. Liu, W. Han, X. Sun, J. Li, J. Shen, Hydrochloric acid pickling process optimization in metal wire working, IJSSST 16 (2015).

[31] M. Ghaffari, M. Ehsani, H.A. Khonakdar, G. Van Assche, H. Terryn, The kinetic analysis of isothermal curing reaction of an epoxy resin-glassflake nanocomposite, Thermochim. Acta 549 (2012) 81–86.

[32] D. Carvalho, C. Joia, O. Mattos, Corrosion rate of iron and iron–chromium alloys in CO_2 medium, Corros. Sci. 47 (2005) 2974–2986.

[33] M.S. Lim, K. Feng, X. Chen, N. Wu, A. Raman, J. Nightingale, E.S. Gawalt, D. Korakakis, L.A. Hornak, A.T. Timperman, Adsorption and desorption of stearic acid self-assembled monolayers on aluminum oxide, Langmuir 23 (2007) 2444–2452.

[34] D. Martin, R. Cole, S. Haq, Investigating the adsorption of oxalic acid onto Cu (110) to create a chemically functionalised surface, Surf. Sci. 539 (2003) 171–181.

[35] G. Socrates, Infrared and Raman Characteristic Group Frequencies: Table and Charts, Ltd. WJS, 2001, pp. 1–347.

[36] M.E. Orazem, B. Tribollet, Electrochemical Impedance Spectroscopy, John Wiley & Sons, 2011.

[37] F. Deflorian, S. Rossi, An EIS study of ion diffusion through organic coatings, Electrochim. Acta 51 (2006) 1736–1744.

[38] F. Mansfeld, C. Tsai, Determination of coating deterioration with EIS: I. Basic relationships, Corrosion 47 (1991) 958–963.

[39] J. Vogelsang, W. Strunz, New interpretation of electrochemical data obtained from organic barrier coatings, Electrochim. Acta 46 (2001) 3817–3826.

[40] E. McCafferty, Introduction to Corrosion Science, Springer, Alexandria, 2010.

[41] B. Hirschorn, M.E. Orazem, B. Tribollet, V. Vivier, I. Frateur, M. Musiani, Determination of effective capacitance and film thickness from constant-phase-element parameters, Electrochim. Acta 55 (2010) 6218–6227.

[42] V.S. Sastri, Green Corrosion Inhibitors: Theory and Practice, John Wiley & Sons, 2012.

[43] R. Naderi, M. Attar, Application of the electrochemical noise method to evaluate the effectiveness of modification of zinc phosphate anticorrosion pigment, Corros. Sci. 51 (2009) 1671–1674.

[44] R. Naderi, M. Mahdavian, M.M. Attar, Electrochemical behavior of organic and inorganic complexes of Zn(II) as corrosion inhibitors for mild steel: solution phase study, Electrochim. Acta 54 (2009) 6892–6895.

[45] A. Kosari, M. Moayed, A. Davoodi, R. Parvizi, M. Momeni, H. Eshghi, H. Moradi, Electrochemical and quantum chemical assessment of two organic compounds from pyridine derivatives as corrosion inhibitors for mild steel in HCl solution under stagnant condition and hydrodynamic flow, Corros. Sci. 78 (2014) 138–150.

[46] A. Amirudin, D. Thieny, Application of electrochemical impedance spectroscopy to study the degradation of polymer-coated metals, Progr. Org. Coat. 26 (1995) 1–28.

[47] F. Mansfeld, M. Kendig, S. Tsai, Evaluation of corrosion behavior of coated metals with AC impedance measurements, Corrosion 38 (1982) 478–485.